Fuel 263 (2020) 116572

Contents lists available at ScienceDirect

Fuel

journal homepage: www.elsevier.com/locate/fuel

Full Length Article

Low salinity water injection in Berea sandstone: Effect of wettability, interface elasticity, and acid and base functionalities

Tomás Eduardo Chávez-Miyauch[a,1], Yingda Lu[a,2], Abbas Firoozabadi[a,b,*]

[a] Reservoir Engineering Research Institute, 595 Lytton Ave., 94301 Palo Alto, CA, USA
[b] Chemical and Biomolecular Engineering Department, Rice University, 70057 Houston, TX, USA

ARTICLE INFO

Keywords:
Enhance oil recovery
Low salinity waterflooding
Contact angle
Interfacial viscoelasticity

ABSTRACT

Injection of low salinity water (LSW) in oil formations may provide improved oil recovery. The mechanisms of the process are not fully understood. There is not clear understanding of what types of crude oil, rock or brine composition lead to improved oil recovery in a secondary or tertiary flooding mode. In this work, five different crude oil samples: three stock tank oils from the Middle East and two obtained by heating the original oils at 55 °C for 24 h are used in waterflooding experiments in Berea sandstone cores. We perform LSW injection in secondary and tertiary mode. Total acid number (TAN), total base number (TBN) of the crude oils, as well as contact angles between rock/oil/brine, and interfacial viscoelasticity between crude oil and brine are measured to shed light into the mechanisms of the process from LSW injection.

In our experiments, there is no increase recovery in tertiary flooding mode, however, there is increased recovery in some of crude oil samples from LSW injection in secondary mode. In one of the three whole crudes, there is significant improved recovery from 53% to 66% by LSW injection in comparison to high salinity water (HSW) injection. In another whole crude, there is no increase in recovery from LSW injection and in the third whole crude, there is limited improved recovery by LSW injection. In both heated crude oils, the recovery is improved significantly; around 10% in one and about 25% in the other from LSW injection compared to HSW injection. The results from recovery are compared to contact angle, interfacial viscoelasticity, TAN, and TBN of the crude oils. There is no strong relationship between wettability alteration (based on contact angle) from LSW injection. We observe correlation with and TBN. The pH of the produced water in our experiments does not depend on the salinity of the injected brine and remains basic at all time (pH = 10). This pH observation is different from the past work in the literature.

1. Introduction

Low-salinity water (LSW) injection has become of intense interest recently. At low salt concentration, the oil recovery may improve in some oil-rock-brine systems. The general belief is that the injection of low-salinity water alters the wettability to a more water-wetting state [1–9].

Recent reviews by Hamon in 2015 [10] and Al-Shalabi & Sepehrnoori in 2016 [11] discuss that there is no clear understanding of LSW injection. There are major differences in the recovery from LSW injection in secondary and tertiary floods. Table 1 lists selected works that show variety of conditions in which the recovery performance has been reported from LSW injection. Both, effectiveness and ineffectiveness of LSW injection in secondary and tertiary flooding mode are reported with no correlation with the rock (outcrop, formation, sandstone, carbonate).

LSW injection in secondary flooding is reported by Nasralla et al. [13] to give 17% higher recovery than injection of connate brine. Zhang & Morrow [15] report LSW injection to give 13.8% higher recovery than HSW injection. Loahardjo et al. [19] report 22.5% higher recovery from LSW injection in comparison to HSW injection.

In tertiary mode, three studies: Austad et al. in 2010 [16]; Cissokho et al. in 2010 [18] and Yousef et al. in 2011 [21] report extra recoveries of 10, 11 and 19.5% from LSW injection, respectively. The extra recovery from tertiary flood may relate to rate effect [22], which can realize in laboratory conditions, as we will discuss later.

The crude oil composition, type of rock, and brine composition, are the main variables that can affect recovery in LSW injection. In this

* Corresponding author.
E-mail address: af@rerinst.org (A. Firoozabadi).
[1] Current address: Universidad La Salle México, Benjamin Franklin 47, 06140 Mexico City, Mexico.
[2] Current address: McDougall School of Petroleum Engineering, The University of Tulsa, 800 South Tucker Drive, 74104 Tulsa, OK, USA.

https://doi.org/10.1016/j.fuel.2019.116572
Received 11 August 2019; Received in revised form 30 October 2019; Accepted 4 November 2019
Available online 21 November 2019
0016-2361/

Table 1
Oil recovery by low salinity water (LSW) injection reported by different authors.

No.	Reference	Rock	Type of Rock	Sow (%)	Injection Sequence*	Secondary Recovery (%OOIP)	Tertiary Recovery (Extra %OOIP)
1	Gamage et al. (2011) [12]	Outcrop	Sandstone (Berea)	32.28	HS-LS	46.58	5.56
		Reservoir	Sandstone (Minelusa)	28.98	HS-LS	39.54	4.00
2	Nasralla et al. (2011) [13]	Outcrop	Sandstone	34.24	CB-DIW	65.00	0.00
				31.47	LS-DIW	79.00	0.00
3	Rivet et al. (2010) [14]	Outcrop	Sandstone	26.40	HS-LS	42.6	0.00
				26.60	LS	45.3	N/A
4	Zhang & Morrow (2006) [15]	Outcrop	Sandstone	21.50	CB-LS	40.60	7.80
				21.70	LS	43.00	N/A
				24.80	HS-LS	58.60	1.30
				24.80	LS	72.40	N/A
5	Austad et al. (2010) [16]	Outcrop	Sandstone	–	HS-LS	50.00	10.00
				–	HS-LS	20.00	15.00
6	Winoto et al. (2012) [17]		Sandstone Outcrop	39.00	HS-LS	30.77	5.77
				43.40	HS-LS	34.74	1.05
				28.10	HS-LS	52.89	0.00
			Carbonate	19.40	HS-LS	39.18	2.06
				20.30	HS-LS	63.19	1.84
				29.20	HS-LS	62.61	0.00
7	Cissokho et. al (2010) [18]	Outcrop	Sandstone	36.00	HS-LS	60.00	11.00
8	Loahardjo et al. (2007) [19]	Reservoir	Sandstone	33.00	HS-LS	57.70	7.60
				26.50	HS-LS	58.10	1.30
				25.20	LS	80.60	N/A
9	Sohrabi et al. (2015) [20]	Reservoir	Sandstone	25.40	HS-LS	50.00	8.10
10	Yousef et al. (2011) [21]	Outcrop	Carbonate	–	HS-LS	67.04	17.93
				–	HS-LS	74.12	19.53

* CB: Connate brine; HS: High salinity, LS: Low salinity, DIW: Deionized Water.

work, only sandstone rock is used.

1.1. Brine composition

Several studies on LSW injection in sandstone have been conducted focusing on the interactions between a variety of rock minerals and clays with crude oils and brines; the brine composition as well as the clay content seem to be the most important variables. Austad et al. [16] have proposed a chemical reaction to explain the release of oil components from the rock surface, which leads to increase in oil recovery. The mechanism has been studied further by RezaeiDoust et al. [23] and Aksulu et al. [24].

The proposed mechanism relies on the ion exchange and negative character of clay in sandstone surfaces, and the ion-exchange power of divalent cations, especially Ca^{2+}. Before water injection at the original conditions, acid and base functional groups in crude oil as well as Ca^{2+} ions from connate water adsorb to clays according to reactions (1–3) below:

$$Clay^- + Ca^{2+} \leftrightarrow Clay^-\cdots Ca^{2+} \quad (1)$$

$$Clay^- + R_3NH^+ \leftrightarrow Clay^-\cdots R_3NH^+ \quad (2)$$

$$Clay^- + R - COOH \leftrightarrow Clay^-\cdots RCOOH \quad (3)$$

When LSW with low content of Ca^{2+} ions is injected, the rock-fluid equilibrium is disturbed. The equilibrium is established from dissociation of water near the surface and protons (H^+) exchange with adsorbed Ca^{2+} ions.

$$Clay^-\cdots Ca^{2+} + H_2O \leftrightarrow Clay^-\cdots H^+ + Ca^{2+} + OH^- \quad (4)$$

As a result, of increase of OH^- ions ad pH increase the stage is set for the acid-base proton transfer reactions.

$$Clay^-\cdots R_3NH^+ + OH^- \leftrightarrow Clay^- + R_3N + H_2O \quad (5)$$

$$Clay^-\cdots RCOOH + OH^- \leftrightarrow Clay^- + RCOO^- + H_2O \quad (6)$$

Then the oil is released from the surface. In their work, Austad et al. [16] present experimental results of adsorption of ions over different clays and pH measurement during coreflooding experiments. The authors observe an increase in pH as wells as increase in oil recovery close to 10% by LSW injection in tertiary mode.

1.2. Oil composition

Crude oil composition may contribute significantly to LSW injection effectiveness. The surface-active components (resins and asphaltenes) in the crude oil interact with the rock and may accumulate at the oil-aqueous phase interface. Acid and base functional groups in the crude oil may interact with the rock leading to the adhesion to the rock surface.

"Total acid number" (TAN) and "total base number" (TBN) quantify the amount of acid functional groups such as naphthenic acids, carboxylic acids and sulphonic acids, and base functional groups such as pyridines, imidazoles and amines in the crude oil. The values are reported as equivalent mg of KOH per gram of the oil.

Table 2 presents TBN and TAN and other relevant crude oil properties as well as the recovery from injection of HSW and connate water in secondary mode followed by low salinity water injection in tertiary mode.

Crude oils of higher asphaltene content do not necessarily show an increase in recovery by LSW injection. Some authors report that a crude oil with a high TAN or TBN may give high oil recovery. According to Shaddel et al. [25], a high TAN/TBN ratio leads to a favorable condition for LSW injection. We have examined the available data and TAN/TBN and recovery from Tables 1 and 2; there is no correlation between the TAN/TBN ratio and oil recovery.

1.3. Flow rate

Injection rate may have a pronounced effect on oil recovery in mixed-wet conditions. In water-wet conditions, when there is no pronounced end effect at high injection rates [22] then there is no significant effect of rate on oil recovery. However, in mixed-wet state the effect of rate on recovery without the end effect can be significant [22]. Laboratory experiments are often conducted at 4–20 PV/day.

Gamage et al. [12] have performed experiments at 0.2 mL/min corresponding to 16 PV/day and report moderate extra recovery in tertiary mode (~5% of original oil in place (OOIP)). Winoto, et al. [17]

Table 2
Oil asphaltene content, TAN and TBN and oil recovery.

No.	Ref.	Asphaltene Content (wt%)	TBN (mg_{KOH}/g_{oil})	TAN (mg_{KOH}/g_{oil})	Injection Sequence Secondary-Tertiary*	Secondary Recovery (%OOIP)	Tertiary Recovery (Additional %OOIP)
1	Gamage et. al. (2011) [12]	10.400	–	–	HS-LS	46.58	5.56
		1.400	0.92	0.074	HS-LS	39.54	4.00
2	Zhang & Morrow (2006) [15]	0.780	1.16	0.33	CB-LS	40.60	7.80
		8.980	2.29	0.17	HS-LS	58.60	1.30
3	Austad (2010) [16]	0.804	0.54	1.82	HS-LS	50.00	10.00
		0.846	1.78	0.12	HS-LS	20.00	15.00
4	Winoto (2012) [17]	6.300	2.49	1.46	HS-LS (sandstone)	30.77	5.77
						34.74	1.05
						52.89	0.00
					HS-LS (carbonate)	39.18	2.06
						63.19	1.84
						62.61	0.00
5	Cissokho (2010) [18]	2.300	0.95	0.17	HS-LS	60.00	11.00
6	Loahardjo (2007) [19]	3.200	1.82	0.16	HS-LS	57.70	7.60
		6.300	2.49	1.46	HS-LS	58.10	1.30
7	Sohrabi (2015) [20]	0.400	4.90	0.35	HS-LS	50.00	8.10
8	Yousef (2011) [21]	5.500	–	0.25	HS-LS	67.04	17.93
				0.25	HS-LS	74.12	19.53

* CB – Connate brine; HS – High salinity and LS – Low salinity.

report several experiments performed at 0.25 mL/min (~18 PV/day). They do not observe significant recovery in tertiary mode. Yousef et al. [21] have performed water flooding at 1–4 mL/min in low permeability carbonate rocks. The rates correspond to about 40–160 PV/day. They observe significant recovery in tertiary mode which may be related to rate effect in mixed-wet conditions. Knowledge of wettability state will help in the interpretation of the results.

1.4. Crude oil-water interfacial properties

Interfacial properties may be affected by salt concentration in the rock-water-oil systems. The increase in the thickness of thin film of water on the rock surface at low salt concentration has been discussed by Nasralla and Nasr-El-Din [6] and by Myint and Firoozabadi [26]. The increase in the thickness of the film of water is related to water-wetting.

Crude oil-water interfacial viscoelasticity may also change from salt amount and composition. Interfacial viscoelasticity is related to shear and deformation. It is related to molecular structure at the interface whereas the interfacial tension is related to the amount of species at the interface [27,28]. The polar components in the crude oil (such as resins and asphaltenes) can form viscoelastic films at the water-oil interface. Alvarado et al. [29,30], Garcia-Olvera et al. [31], and Chávez, Firoozabadi and Fuller [32] have discussed the effect on oil recovery from oil-water interface viscoelasticity.

Alvarado et al. [29,30] correlate the extra oil recovery from LSW injection to the viscoelasticity at the fluid–fluid interface. The authors report a maximum elastic modulus of 38 mN/m at a brine concentration of 6.724 mM Na_2SO_4 (0.95 g/L). At this brine concentration, the oil recovery from coreflooding is 20% higher than that at a higher salinity of 672.4 mM (95 g/L) where elastic modulus is smaller. The authors suggest that the elasticity of the fluid-fluid interface affects oil recovery by reducing the oil snap-off in the displacement. They also observe that oil droplets generated in a microfluidic device are larger in low salinity than in high salinity.

Chavez, Firoozabadi and Fuller [32] present a systematic study of non-monotonicity of the fluid–fluid interface as a function of salt concentration. There is a substantial increase in fluid–fluid elasticity at low salinities. The authors also report a decrease in the viscoelastic moduli but an increase in the elastic character of the interface when a small amount of a non-ionic surfactant is added to the water. An increase of 10% in oil recovery is observed in the micromodel waterflooding experiments in more elastic interfaces (low salinity and surfactant addition).

Some of the functional components in the crude oil, and ions in brine may have significant effect on fluid-fluid interfacial rheology. Garcia-Olvera, et al. [31] report the change of the crude oil-brine interfacial viscoelasticity by asphaltene fractions and by acids. They observe an increase in interfacial viscoelasticity as the fraction of asphaltenes increases and a decrease with increase in naphthenic acids.

In this work we investigate the relationship between improved oil recovery from LSW injection as a function of crude oil composition in fired Berea sandstone. The firing process reduces the effect from clay contribution, which has been argued as the most important element in LSW injection experiments. We use three different crude oils and heat two of them to perform a comprehensive investigation of the oil properties that affect LSW injection. Along with the recovery and pressure drop measurements, we also analyze the salt concentration in the produced water as well as the pH of the produced water. We keep the flow rate, brine composition, and rock type the same to focus on oil properties and salt concentration of injected water. In two of the crude oils, we observe an increase in oil recovery by LSW injection in comparison to HSW injection in secondary mode. The pH of the produced water is observed to remain basic at all times, and there is no significant difference in pH of the produced water in HSW and LSW injection. We measure TAN and TBN of all the five crudes to correlate recovery to acid and base functionalities. We also perform contact angle measurements, and interfacial viscoelasticity to analyze the effect of salt concentration.

2. Materials and methods

2.1. Fluids

We used five different crude oil samples in this work: three stock tank oils (K1, K2, and K3) from the Middle East, and a variation of crude oils K1 and K2, by heating at 55 °C under continuous stirring overnight. Heated oils are designated as K1H and K2H. To avoid vaporization of light components in waterflooding with stock oils, the system is pressurized, and the backpressure is maintained at 100 psi during the test. In coreflooding of the heated oils, there is no need to use a backpressure regulator at high pressure. Properties of the whole and heated oils are listed in Table 3. Density and viscosity of oil samples are measured by an Anton Paar DMA5000 density meter, and an Anton Paar MCR 302 shear rheometer with 50-mm parallel plate geometry, respectively. All devices are calibrated using DI water, air and reference

Table 3
Relevant properties of the three whole and heated crudes at 25 °C.

Oil	ρ (g/mL)	μ (cP)	TAN (mg_{KOH}/g)	TBN (mg_{KOH}/g)
K1	0.870 ± 0.010	9.90 ± 0.48	0.075 ± 0.002	0.923 ± 0.017
K1H*	0.913 ± 0.010	50.08 ± 0.02	0.124 ± 0.003	1.132 ± 0.050
K2	0.852 ± 0.009	7.83 ± 0.36	0.078 ± 0.001	0.650 ± 0.066
K2H*	0.888 ± 0.001	25.04 ± 0.27	0.104 ± 0.004	0.954 ± 0.015
K3	0.825 ± 0.004	5.66 ± 0.35	0.074 ± 0.002	0.527 ± 0.021

* Heated oils K1 and K2, respectively.

Table 4
Brines composition.

Salt	Salt Concentration (wt%)		
	Connate Water	High Salinity Water (HSW)	Low Salinity Water (LSW)
NaCl	13.79	4.00	0.10
KCl	0.41	–	–
$CaCl_2$	3.68	–	–
$MgCl_2$	0.89	–	–
Na_2SO_4	0.08	–	–

fluids prior to performing the measurements.

TAN and TBN are measured based on the ASTM methods by performing potentiometric titrations. Measurements are repeated from 3 to 5 times.

The brines are prepared by mixing salts in DI water. Connate water is prepared based on the composition of the reservoir brine. High salinity and low salinity brines are from NaCl solutions. Compositions of the brines are presented in Table 4.

2.2. Core samples

Berea sandstone cores of 1.5 in diameter and 5.5 in length are used in all water injection floodings. Cores are fired at 850 °C for a period of 12 h. Firing is performed to stabilize the clays and minimize clay swelling in waterflooding as reported by Wu and Firoozabadi [33] and by Rezaei and Firoozabadi [34]. The firing increases the porosity and permeability of the cores.

Typical mineralogy of Berea before and after firing has been reported in the literature [35,36]. The composition is listed in Table 5. Note that there is significant decrease in clay content (Kaolinite and Illite) from firing.

In our work, only fired Berea cores are used. The major mineral is quartz, which has similar behavior in contact angle to mica [37]. Mica is used in this work in contact angle measurements.

2.3. Experimental procedure

2.3.1. Core saturation

A schematic of the waterflooding setup is shown in Fig. 1. All cores are prepared following the same procedure. Each core is cleaned by injecting 2–3 PV of isopropyl alcohol, and then dried in the oven at 120 °C for 10 h to remove solvent residuals.

The clean core is placed in a metal core-holder connected to vacuum to evacuate trapped air. Dead volume of the fittings was determined by flowing water through them at constant flow rate and determining the time of filling. The dead volume of the fittings is 0.8 mL. The core is saturated with brine with the core evacuated. We flow 2 PV and then an extra PV with the outlet open to atmospheric pressure to determine permeability and porosity Once we observe water at the core outlet the vacuum is stopped. We assume that after 3 PV the brine inside the core has reached the concentration of connate brine. Dead volume is considered for determination of permeability and porosity. After 3 PV injection, the outlet valve is closed, pressurized to 100 psi and aged for 4 days.

After aging with brine, crude oil is injected at a rate of 5 PV/day until there is no water produced. Backpressure is kept at 100 psi with the use of a low volume pressure regulator. The system is then closed, pressurized to 100 psi and aged for 2 weeks before performing waterflooding tests. Data of the saturated cores are listed in Table 6.

Table 5
Berea sandstone composition.

Mineral	Berea (wt%) Churcher et al. 1991 [33]	Fired Berea (wt%) Shouxiang & Morrow 1994 [34]
Quartz	87.0	87.9
Feldspar	4.0	1.7
Dolomite	2.0	0.0
Kaolinite	6.0	1.3
Illite	1.0	–
Chert	–	1.3
Calcium Oxide	–	3.9
Rock Fragments	–	3.9

2.3.2. Waterflooding procedure

Two types of coreflooding are performed; in one, LSW is injected in the secondary mode, in the other, HSW is injected first followed by LSW injection. The injection rate is 5 PV/day. Pressure is recorded at the inlet of the core. The outlet is connected to a backpressure regulator and the pressure is maintained at 100 psi for crude oils K1, K2 and K3. For crude oils K1H and K2H, the outlet is open to atmospheric pressure.

At the end of all tests, flow rate is increased to 25 PV/day to examine the end effect, and wettability state [22]. When there is no end effect, additional oil recovery is due to mixed-wetting conditions [22] from the increase in flow rate. During the tests, samples of produced water are collected. pH is measured using pH paper strips and then dried in the oven to determine the salt concentration in the produced water. Paper pH strips are selected because of simplicity and because it can give a direct value with a small sample volume to facilitate examination of variations in the pH of the produced water. We do not use a pH meter because it requires a large amount of water. In order to quantify the accuracy of pH measurements by the pH strips we made three measurements in different buffer solutions of known pH and compared with accurate measurements by a pH meter. The accuracy is ± 0.5.

2.3.3. TAN and TBN measurements

TAN and TBN measurements are performed according to the ASTM D664 and ASTM D2896-11 methods, respectively. In both we modified the solvent mixture with toluene. The measurements are performed using an automatic titration system, Metrohm 916 Ti-Touch with a combined pH glass electrode for non-aqueous media.

2.3.4. Contact angle measurements

We performed contact angle measurements by placing an oil droplet on the surface of a mica slide as described by Aslan et al. [37]. Briefly, about 500, mL of prepared brine solution is loaded into a square-shape glass beaker. The substrate slide, supported by a customized stainless-steel holder, is submerged in the brine solution for 1 h. The aging time is adequate for the substrate slide to equilibrate with brine. We place the needle tip close to the bottom surface of substrate slide, and slowly dispense 100-μL of oil. The oil droplet would touch the bottom of substrate slide once it reaches a certain size. At the end of the dispensing process, we gently move the needle downward, leaving the oil droplet to stay on the bottom surface of the substrate slide. The droplet is allowed to equilibrate for 3 days before measurements are taken. The droplet images are captured using a 12X ThorLabs camera; then analyzed by an ImageJ program “DropSnake” to obtain contact angle [38,39]. Four droplets are placed on the surface of the mica slide at

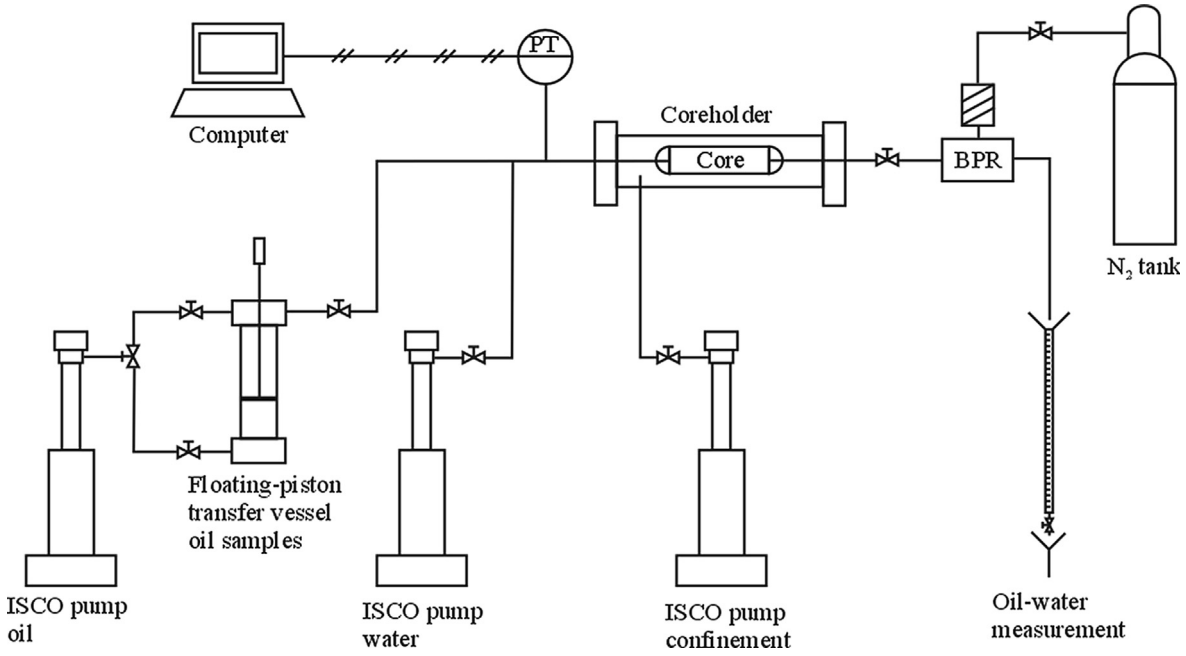

Fig. 1. Experimental setup for waterflooding experiments.

Table 6
Relevant core properties in different tests.

Core	Oil	Injection Water*	PV (mL)	Φ** (%)	k_W** (mD)	OOIP (mL)	S_{WI} (%)
A1	K1	HS-LS	33.84	20.16	70.6	22.5	33.51
A2	K1	HS-LS	30.23	20.88	68.2	21.0	30.53
A3	K1	LS	29.97	19.50	75.2	20.0	33.27
A4	K1	LS	30.40	21.40	71.8	22.0	27.63
B1	K1H	HS-LS	30.73	19.29	62.9	21.5	30.03
B2	K1H	HS-LS	29.24	19.62	43.2	21.5	26.47
B3	K1H	LS	34.96	21.33	76.6	21.0	42.79
B4	K1H	LS	27.08	18.30	61.3	19.0	29.83
C1	K2	HS-LS	30.70	20.28	67.2	21.0	31.60
C2	K2	HS-LS	29.55	20.58	69.8	20.0	32.43
C3	K2	LS	31.13	21.39	60.3	20.5	34.15
C4	K2	LS	29.60	20.55	71.5	20.5	30.63
D1	K2H	HS-LS	30.15	19.89	60.6	19.9	34.00
D2	K2H	HS-LS	32.59	20.33	66.9	22.3	31.57
D3	K2H	LS	31.60	21.13	40.4	22.0	36.42
D4	K2H	LS	31.02	20.09	61.4	21.0	36.36
E1	K3	HS-LS	31.65	20.87	69.8	20.5	35.23
E2	K3	HS-LS	32.27	20.83	76.8	21.5	33.37
E3	K3	LS	30.25	20.32	66.7	20.00	33.88
E4	K3	LS	31.13	20.09	64.9	20.50	34.15

* HS – High salinity and LS – Low salinity.
** Porosity and absolute permeability by connate brine are obtained when saturating the core.

each run and we report the results by average and standard deviation. Mica contact angle measurements relate to sandstone contact angle as mentioned above.

2.3.5. Interfacial viscoelasticity measurements

Crude oil – brine interfacial viscoelasticity measurements are performed using an Anton Paar MCR 302 shear rotational rheometer adapted to a du Noüy ring. Interfacial properties are measured by applied stress (σ), and strain response (γ) in terms of the frequency of oscillations (ω) [38], σ_0 and γ_0 are the stress and strain at the maximum:

$$G^* = \frac{\sigma_0}{\gamma_0} \exp[i \cdot \delta(\omega)] \quad (4)$$

The complex modulus G^* can be split into two components:

$$G^* = G'(\omega) + iG''(\omega) \quad (5)$$

where G' is the storage or elastic modulus related to the elastic character, G'' is the loss or viscous modulus related to the viscous character of the interface and δ is the phase angle which is a direct measure of the viscous and elastic character of the interface ($\delta = 0^\circ$ interface is elastic while $\delta = 90^\circ$ interface it is viscous). In each experiment, the sample cell is cleaned using wipes soaked in chloroform and dried with clean wipes and dry air. The DuNoüy ring is cleaned by soaking into chloroform, then fired to remove any residue and allowed to cool down to room temperature. Constant oscillation tests are performed at room temperature (20 °C) with small strain amplitude (1.0%), and frequency (0.5 rad/s). Oscillations are performed each 15 min. Data is collected after stabilization at 24 h. The evolution of the storage elastic modulus (G') and loss viscous modulus (G'') are analyzed as well as the phase angle (δ).

3. Results

3.1. Waterflooding performance

Waterflooding experiments are duplicated to improve reliability to be able to draw firm conclusions. In every coreflooding test a new core is used. In a typical HSW injection, we inject 10 pore volumes of water followed by injection of 5 pore volumes of LSW at 5 PV/day. We increase the injection rate at the end to 25 PV/day to examine the end effect. All tests show no significant extra recovery from LSW injection in tertiary mode. In a secondary LSW injection test, we inject 10 pore volumes of water at 5 PV/day and we increase the rate at the end to 25 PV/day. There is no extra recovery either in LSW or HSW toward the end of the test when the flow rate is increased, which is an indication of negligible end effect, and water-wetting state [22].

Pressure profile is similar in all flooding tests. Pressure stays nearly constant until breakthrough. After breakthrough, it decreases and then remains constant. Pressure fluctuations seem to be higher in HSW in comparison to LSW, however, the difference is not significant. By increasing the flow rate, the pressure drop increases but not in proportion to flow rate increase. At high rate, there may be fingering. There may be small amount of emulsion formation, which can also affect pressure drop from increase in injection rate.

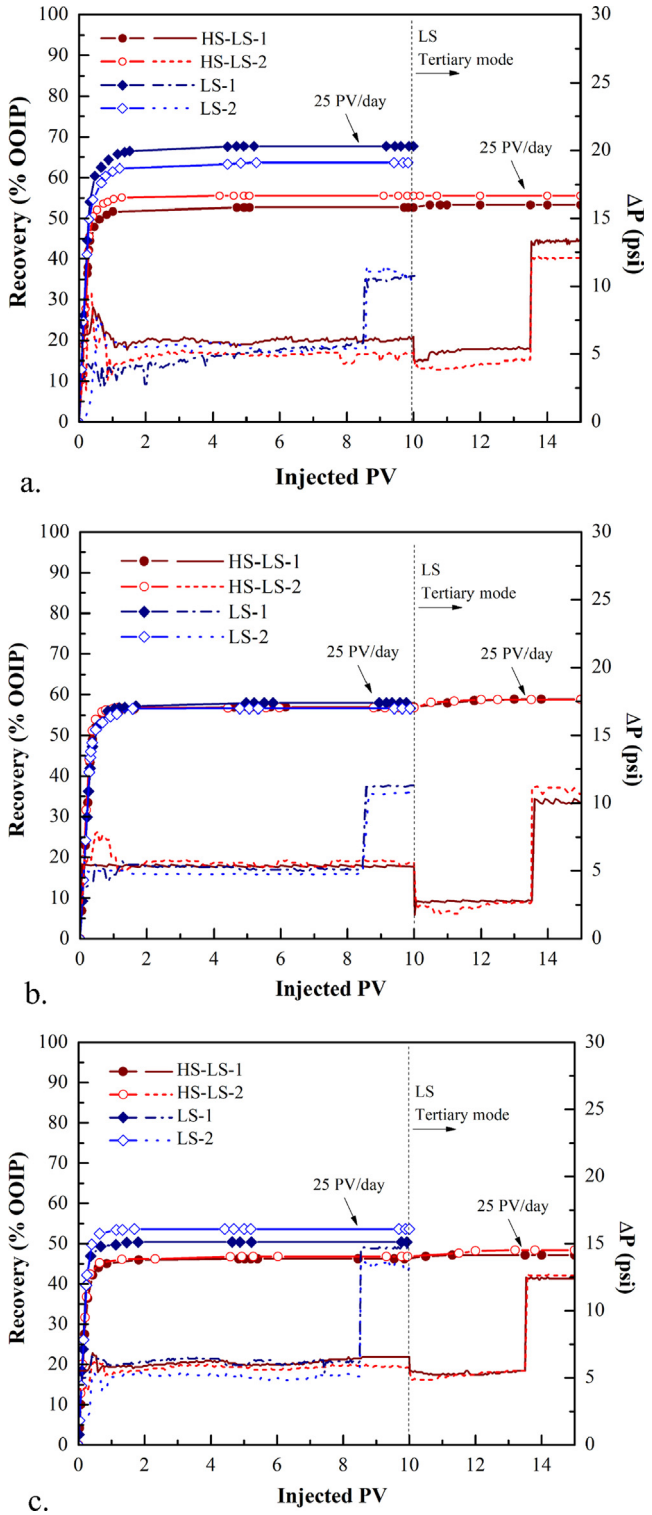

Fig. 2. Recovery performance and pressure drop in water flooding from LSW and HSW injection in three different oils: a. K1, b. K2 and c. K3.

3.2. Recovery performance from HSW and LSW injection

Results of crude oils K1, K2 and K3 are plotted in Fig. 2. Note that when there is flow rate increase there is also a sharp increase in pressure drop. Extra recovery from injecting LSW in tertiary mode for the three oils is practically zero. There is also no extra recovery when increasing the flow rate 5 times at the end of the experiments. In the secondary mode, there is increase in recovery from LSW injection in oil

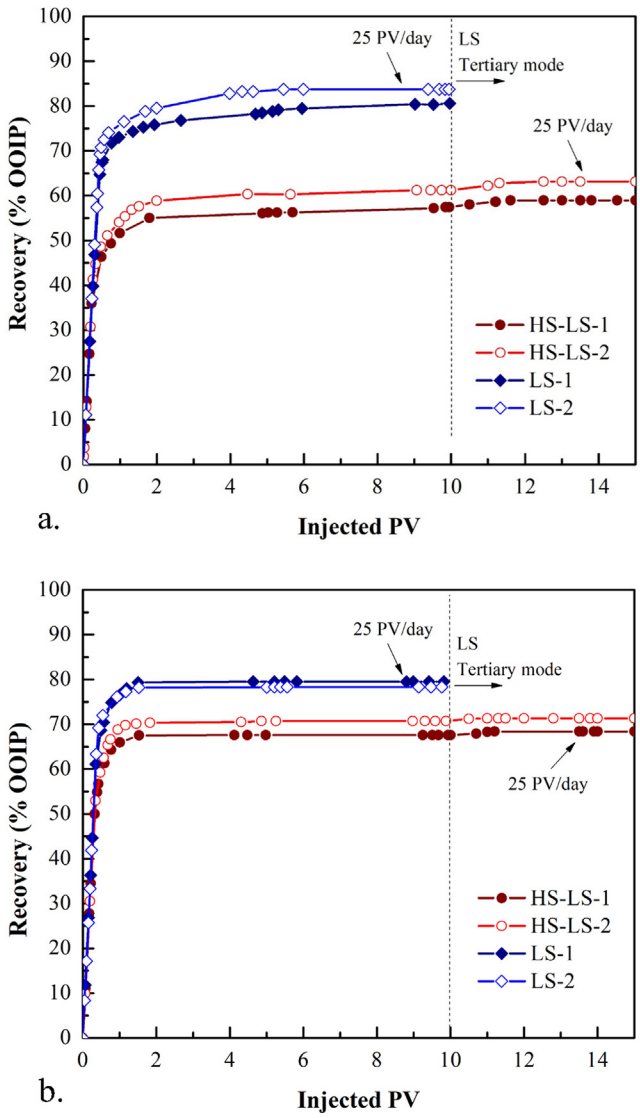

Fig. 3. Recovery performance in LSW and HSW injection of heated oils: a. K1H, and b. K2H.

K1. The salinity effect is pronounced in oil K1 where recovery is in average about 12% higher in LSW than in HSW, while in oil K3, recovery with LSW is in average about 4% higher than in HSW. The effect is very small in oil K2. There is no relation between the μ_o/μ_w ratio and recovery in these oils.

When the oils are heated, light components are removed. The LSW effect in secondary waterflooding in heated oils becomes pronounced. Recovery performance of the oils K1H and K2H are depicted in Fig. 3.

Recovery from LSW injection is about 22% higher than HSW injection in the K1H oil. LSW injection in oil K2H is about 10% higher than HSW injection. Note that in the whole oil K2 there is no increase in recovery from LSW injection as shown in Fig. 2. The recovery from HSW injection in oil K2 is higher than HSW injection in oils K1 and K3. Oil K3 has the lowest recovery from HSW injection.

3.3. pH and salt concentration of produced water

We mixed powders of Berea rock with connate water and injection water. The. pH of the supernatant was measured using pH paper. When mixing Berea powder (fired and unfired) with connate water, the pH remained neutral (7.5) while when Berea powder was mixed with injection water (HSW and LSW), pH was basic (9.5 and 10, respectively).

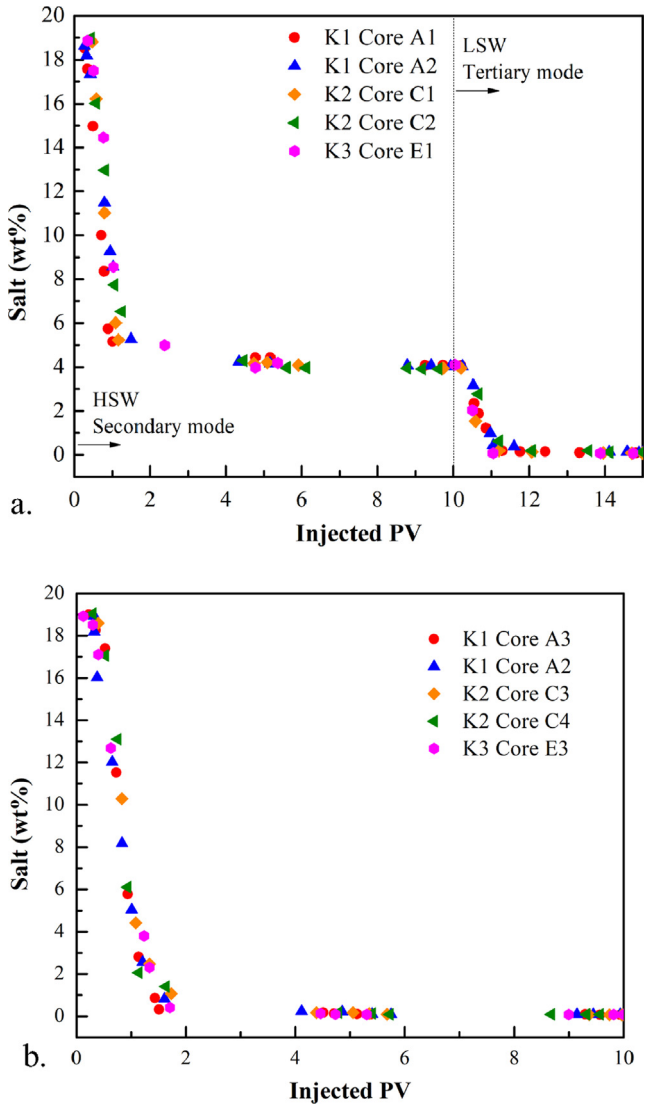

Fig. 4. Salt concentration of produced water in various corefloodings in the three oils: a. HSW followed by LSW and b. LSW.

pH may be affected by the interaction of water with the clays in Berea sandstone. In connate water, there may be less dissolution of ions from the rock.

pH and salt concentration of the produced water are measured in all tests. pH remained basic (10 – 10.5) regardless of the type of injection water. RezaeiDoust et al. [23], suggest that the basic pH may give extra recovery and would be from the interaction between clay and LSW. However, our pH data show the recovery does not correlate with pH.

Fig. 4 shows that the salt concentration of the produced water varies due to the mixing of connate water and injection water. The substantial decrease in the salt concentration from breakthrough to about 1.5 PV is likely caused by the mixing of connate water and injection water. Apparently, the high salt connate water is substituted with low salt concentration of injection water.

3.4. Contact angle measurements

Contact angle is measured to evaluate wettability. Aslan, Najafabadi and Firoozabadi [37] report the non-monotonic behavior of the contact angle of two petroleum fluids on mica and quartz surfaces as a function of NaCl and $MgCl_2$ concentration. Jimenez and Firoozabadi [40] report the results from molecular dynamics simulations and show the variation of the contact angle to be due to the ionic structures in the thin film formed between the oil droplet and the substrate. To shed light on the results from waterflooding tests, contact angle measurements are performed in mica plates and HSW/LSW. Results are summarized in Table 7.

Table 7
Contact angle measurements (degrees).

Crude Oil	Brine	
	HSW	LSW
K1	22.97 ± 0.53	21.31 ± 0.73
K1H	39.37 ± 0.43	21.07 ± 1.03
K2	19.53 ± 0.83	18.79 ± 0.71
K2H	19.74 ± 0.86	18.92 ± 0.29
K3	18.36 ± 1.30	17.59 ± 1.58

The contact angle is around 20° except for the heated oil K1H/HSW which is about 40°, indicating somewhat less water wetting. For K1H, the contact angle measured in HSW is 20° higher than that in LSW and this trend correlates with the higher oil recovery from LSW injection. There is no appreciable difference in contact angle between HSW and LSW in oils K1, K2, K2H and K3, suggesting that wettability alteration may not be a factor in the difference in oil recovery in these oils. In the contact angle measurements, we first expose the substrate to the aqueous phase based on the idea that a rock in the formation is first exposed to water and then there is oil migration (see Table 7).

3.5. Interfacial viscoelasticity of crude oil – water interface

There is not much difference in contact angle from oils K1, K2 and K3 with LSW and HSW. However, these two oils respond differently to LSW injection. Interfacial viscoelasticity measurements are performed to examine the effect of interface elasticity on oil recovery in addition to wettability. Elastic modulus (G'), viscous modulus (G'') and phase angle (δ) of the corresponding interfaces are listed in Table 8. The data are at time = 24 h where the interface has fully developed. The interfaces of oil with LSW show higher elasticity than the ones formed in contact with HSW. The phase angle is about 29° for the oil K1-LSW interface while it is about 37° at the interface of oil K1-HSW. The smaller phase angle indicates a higher interface elasticity. For the interface of oil K2-brine interface the phase angles are about 29° and 32° for the LSW and HSW, and for oil K3, the phase angles are 31° and 32° respectively. As with the case of the contact angle, only oil K1 shows a difference in viscoelasticity between LSW and HSW. The other phase angles from LSW and HSW are close.

When analyzing the elastic modulus (G'), the interfaces show different behavior from salt concentration. G' is about 20 mN/m for the interface of oil K1-HSW and about 81 mN/m for the interface of oil K1-LSW. For oil K2, G' is 21 mN/m with HSW and 58 mN/m with LSW and for oil K3 G' is 4.7 mN/m with HSW and 21 mN/m with LSW. G' for interfaces formed with oils K1 and K3 with LSW are about 4 times larger than interfaces formed with HSW, while with oil K2 G' with LSW is less than 3 times the modulus formed with HSW. The increase in elastic modulus can be related to an increase in the strength of the

Table 8
Interfacial viscoelasticity.

Crude oil	Brine	G' (mN/m)	G'' (mN/m)	δ (deg)
K1	LSW	81.3	40.4	29.4
K1	HSW	20.2	15.1	36.8
K2	LSW	58.3	32.8	29.3
K2	HSW	21.3	13.5	32.3
K3	LSW	21.1	12.5	30.6
K3	HSW	4.7	2.9	32.2

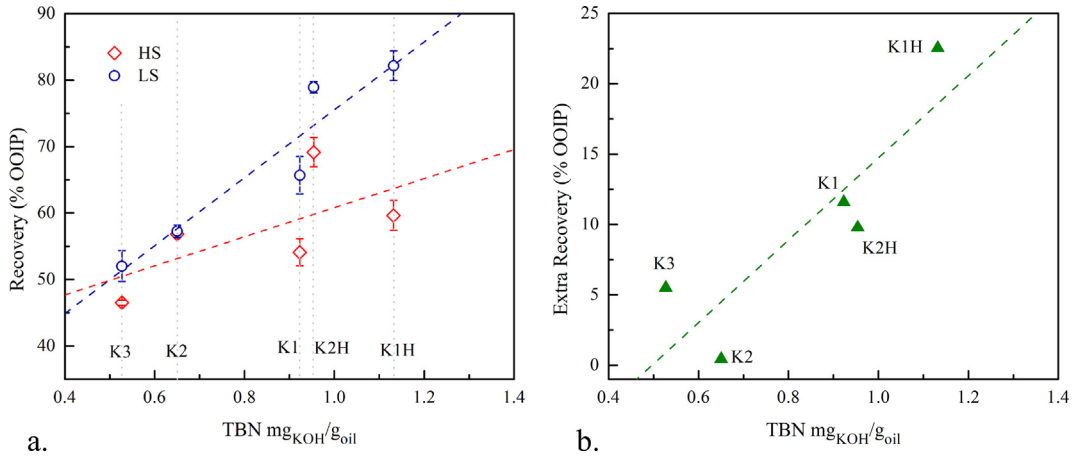

Fig. 5. a. Secondary recovery vs TBN in HSW and LSW injection. b. Extra recovery from LSW injection (over HSW injection) vs TBN.

interface and is in line with the increase in recovery. We should comment that the changes in the interface elasticities are not significant in terms of phase angle except for oil K1. Methods other than the use of du Noüy ring may give results that are more accurate when phase angles are close.

3.6. TAN and TBN correlation with recovery

The contact angle and the interfacial viscoelasticity are consequence of accumulation and structure at the interfaces, respectively. In contact angle, the acid and base functionalities of the oil with the minerals on the rock surface and in interfacial viscoelasticity, the accumulation and structure of acid and base functional groups of the oil on the water-oil interface are key elements.

We therefore examine correlation of oil recovery in secondary mode with TBN in HSW and LSW injection (TAN range between the five crudes is too short to perform a correlation). Fig. 5 presents a plot of oil recovery from LSW and HSW injection in secondary mode vs TBN and the difference in recovery between LSW and HSW in secondary mode.

The data show a correlation between TBN in both HSW and LSW injection. This correlation is in line with the efficiency of LSW injection in secondary mode (extra recovery between HSW and LSW).

4. Concluding remarks

In this work we have used five different crude oils to examine the effect of LSW injection on oil recovery in Berea sandstone. In four of the crudes there is very little difference in contact angle from the salt concentration in the injected water. In one crude the salt concentration of the injected water affects contact angle; the contact angle is about 40° at 4 wt% NaCl concentration and reduces to about 20° at 0.1 wt% NaCl concentration.

The following conclusions are drawn from this work:

- LSW injection in the water-wetting state does not give extra recovery after HSW injection implying no benefit from LSW injection in tertiary mode. The direct evidence from water-wetting is that there is no additional recovery from injection rate increase by a factor of five.
- Contact angles of crude oil-brine-mica reveal that the substrates are preferentially water-wet and that there is no significant difference in wettability between HSW and LSW except for one of the two heated oils with the highest TAN and TBN.
- Produced water has high pH, perhaps because of dissolution / ion exchange in clays. There is no difference in pH of produced water from LSW and HSW injection in our experiments.
- Salt concentration of produced water decreases due to the mixing of injected brine and connate water. Produced water has the salt concentration of the injected water after 1 to 1.5 PV from breakthrough. This may be also an indication that the rock is water-wet because the water mixing is gradual during the flooding.
- Interfacial viscoelasticity data indicate that interface elasticity and effectiveness of LSW injection may be related. The increase in storage modulus $\acute{G}$ (4 times for oils with LSW) and the decrease in phase angle δ relate to the formation of an elastic interface that can deform during waterflooding, avoiding snap-off.
- Recovery from LSW in secondary mode correlates with the base functionalities in the oil. Base components adsorb preferably to the crude oil-water interface leading to a more elastic interface.

Declaration of Competing Interest

The authors declare that they have no known competing financial interests or personal relationships that could have appeared to influence the work reported in this paper.

Acknowledgements

We thank the Kuwait Oil Company and other members of the RERI research consortium for funding the work. T.C. acknowledges generous support from the Mexican Council of Science and Technology (CONACYT) for the postdoctoral scholarship for research work at RERI.

References

[1] Tang GQ, Morrow NR. Influence of brine composition and fines migration on crude oil/brine/rock interactions and oil recovery. J Petrol Sci Eng 1999;24:99–111.
[2] Morrow NM, Buckley J. Improved oil recovery by low-salinity waterflooding. J Petrol Technol Distinguished Authors Series 1999:SPE-129421.
[3] Lager A, Webb KJ, Black CJ, Singleton M, Sorbie KS. Low salinity oil recovery – an experimental investigation. 2006, SCA2006-36.
[4] Sorbie KS, Collins I. A proposed pore-scale mechanism for how low salinity waterflooding works. 2010, SPE 129833-MS.
[5] Hadia N, Lehne H, Kumar K, Selboe K, Stensen J, Torsæter O. Laboratory investigation of low salinity waterflooding on reservoir rock samples from the Frøy field. 2011, SPE 141114.
[6] Nasralla RA, Nasr-El-Din HA. Double layer expansion: is it a primary mechanism of oil improved oil recovery by low-salinity waterflooding? SPE Reservoir Eval Eng 2014;17:49–59.
[7] Omekeh AV, Friis HA, Fjelde I, Evje S. Modeling of ion-exchange and solubility in low salinity water flooding. 2012, SPE 154144-MS.
[8] Zahid A, Shapiro AA, Skauge A. Experimental studies of low salinity water flooding carbonate. 2012, SPE 155625-MS.
[9] Lee SY, Webb KJ, Collins IR, Lager A, Clarke SM, O'Sullivan M, Routh AF, Wang X. Low salinity oil recovery-increasing understanding on the underlying mechanisms. 2010, SPE-129722.
[10] Hamon G. Low salinity waterflooding: facts, inconsistencies and way forward. 2015, SCA 2015-Temp Paper.
[11] Al-Shalabi E, Sepehrnoori K. A comprehensive review of low salinity/engineered

water injections and their applications in sandstone and carbonate rocks. J Petrol Sci Eng 2016;139:137–61.
[12] Gamage P, Thyne G. Comparison of oil recovery by low salinity waterflooding in secondary and tertiary modes. 2011, SPE 147375-MS.
[13] Nasralla R, Alotaibi M, Nasr-El-Din H. Efficiency of oil recovery by low salinity water flooding in sandstone reservoirs. 2011, SPE 144602-MS.
[14] Rivet S, Lake L, Pope G. A coreflood investigation of low salinity enhanced oil recovery 2010, SPE 134297.
[15] Zhang Y, Morrow N. Comparison of secondary and tertiary recovery with change in injection brine composition for crude oil/sandstone combinations. 2006, SPE 99757-MS.
[16] Austad T, RezaeiDoust A, Puntervold T. Chemical mechanism of low salinity water flooding in sandstone reservoirs. 2010, SPE 129767.
[17] Winoto W, Loahardjo N, Xie X, Yin P, Morrow NR. Secondary and tertiary recovery of crude oil from outcrop and reservoir rocks by low salinity waterflooding. 2012, SPE 154209-MS.
[18] Cissokho M, Boussour S, Cordier P, Bertin H, Hamon G. Low salinity oil recovery on Clayey sandstone: experimental study. Petrophysics 2010;51(5):305–13.
[19] Loahardjo N, Xie X, Yin P, Morrow N. Low salinity waterflooding of a reservoir rock. 2007, SCA 2007-29.
[20] Sohrabi M, Mahzari P, Farzaneh S, Mills J, Tsolis P. Novel insights into mechanisms of oil recovery by low salinity water injection. 2015, SPE 172778-MS.
[21] Yousef AA, Al-Saleh S, Al-Kaabi A, Al-Jawfi MS. Laboratory investigation of the impact of injection-water salinity and ionic content on oil recovery from carbonate reservoirs. SPE Res Eval Eng 2011;14(05). SPE 137634 PA.
[22] Tang GQ, Firoozabadi A. Effect of pressure gradient and initial water saturation on water injection in water-wet and mixed-wet fractured porous media. SPE Reservoir Eval Eng 2001;4(06):516–24.
[23] RezaeiDoust A, Puntervold T, Austad T. Chemical verification of the EOR mechanism by using low saline/smart water in sandstone. Energy Fuels 2011;25:2151–62.
[24] Aksulu H, Håmsø D, Strand S, Puntervold T, Austad T. Evaluation of low-salinity enhanced oil recovery effects in sandstone: effects of the temperature and pH gradient. Energy Fuels 2012;26:3497–503.
[25] Shaddel S, Tabatabae-Nejad SA, Fathi SJ. Low salinity water flooding: Evaluating the effect of salinity on oil and water relative permeability, wettability and oil recovery. Special Topics and Reviews in Porous Media 2014;5(02):1–33.
[26] Myint PC, Firoozabadi A. Thin liquid films in improved oil recovery from low-salinity brine. Curr Opin Colloid Interface Sci 2015;20:105–14.
[27] Fuller GG. Rheology of Mobile Interfaces. Rheology Reviews, 2003, ed DM Binding and K Walters (Aberystwyth: The British Society of Rheology), 77–124.
[28] Lucassen-Reynders EH. Interfacial viscoelasticity in emulsions and foams. Food Struct 1993;12(1):1–12.
[29] Alvarado V, Bidhendi MM, García-Olvera G, Morin B, Oakey JS. Interfacial Visco-Elasticity of Crude Oil-Brine: An Alternative EOR Mechanism in Smart Waterflooding. 2014, SPE 169127-MS.
[30] Alvarado V, Bidhendi MM, García-Olvera G, Morin B, Oakey JS. Interfacial visco-elasticity of crude oil-brine: an alternative EOR mechanism in smart waterflooding. SPE J 2018;23(03):803–18.
[31] Garcia-Olvera G, Reilly TM, Lehmann TE, Alvarado V. Effects of asphaltenes and organic acids on crude-oil brine interfacial visco-elasticity and oil recovery in low salinity waterflooding. Fuel 2016;185:151–63.
[32] Chavez-Miyauchi TE, Firoozabadi A, Fuller GG. Non-monotonic elasticity of the crude oil-brine interface in relation to improved oil recovery. Langmuir 2016;32(9):2192–8.
[33] Wu S, Firoozabadi A. Effects of firing and chemical treatments on Berea permeability and wettability. Energy Fuels 2011;25:197–207.
[34] Rezaei N, Firoozabadi A. Pressure evolution and production performance of waterflooding in n-heptane saturated fired Berea cores. SPE J 2014;19(04):674–86.
[35] Churcher PL, French PR, Shaw JC, Schramm LL. Rock properties of Berea sandstone, Baker dolomite, and Indiana limestone. 1991, SPE-21044.
[36] Shouxiang M, Morrow N. Effect of firing on petrophysical properties of Berea sandstone. SPE Form Eval 1994;9(03):213–8.
[37] Aslan S, Najafabadi NF, Firoozabadi A. Non-monotonicity of contact angle from NaCl and $MgCl_2$ concentrations in two petroleum fluids on atomistically smooth surfaces. Energy Fuels 2016;30:2858–64.
[38] Stalder AF. DropSnake and LB-ADSA 2006 user manual. École Polytechnique Fédérale de Lausanne.
[39] Stalder AF, Kulik G, Sage D, Barbieri L, Hoffmann P. A snake-based approach to accurate determination of both contact points and contact angles. Coll Surf A: Physicochem Eng Aspects 2006;286:92–103.
[40] Jimenez-Angeles F, Firoozabadi A. Tunable substrate wettability by thin water layer. J Phys Chem C 2016;120(43):24688–96.